DAF-16/FOXO and EGL-27/GATA promote developmental growth in response to persistent somatic DNA damage

Published in final edited form as:
Nat Cell Biol. 2014 December ; 16(12): 1168–1179. doi:10.1038/ncb3071.

DAF-16/FoxO and EGL-27/GATA promote developmental growth in response to persistent somatic DNA damage

Michael M. Mueller[#1,2], **Laia Castells-Roca**[#1,2], **Vipin Babu**[1,2], **Maria A. Ermolaeva**[1,2], **Roman-Ulrich Müller**[2,3], **Peter Frommolt**[2,4], **Ashley B. Williams**[1,2], **Sebastian Greiss**[2,6], **Jennifer I. Schneider**[1,2], **Thomas Benzing**[2,3], **Bernhard Schermer**[2,3], and **Björn Schumacher**[1,2,*]

[1]Institute for Genome Stability in Ageing and Disease, Medical Faculty, University of Cologne, Joseph-Stelzmann-Str. 26, 50931 Cologne, Germany

[2]Cologne Excellence Cluster for Cellular Stress Responses in Aging-Associated Diseases (CECAD) Research Center and Systems Biology of Ageing Cologne, University of Cologne, Joseph-Stelzmann-Str. 26, 50931 Cologne, Germany

[3]Department II of Internal Medicine and Center for Molecular Medicine Cologne, University of Cologne, 50937 Cologne, Germany

[4]Cologne Center for Genomics, University of Cologne, Weyertal 115b, 50931 Cologne, Germany

[#] These authors contributed equally to this work.

Abstract

Genome maintenance defects cause complex disease phenotypes characterized by developmental failure, cancer susceptibility, and premature aging. It remains poorly understood how DNA damage responses function during organismal development and maintain tissue functionality when DNA damage accumulates with aging. Here we show that the FoxO transcription factor DAF-16 is activated in response to DNA damage during development while the DNA damage responsiveness of DAF-16 declines with aging. We find that in contrast to its established role in mediating starvation arrest, DAF-16 alleviates DNA damage-induced developmental arrest and even in the absence of DNA repair promotes developmental growth and enhances somatic tissue functionality. We demonstrate that the GATA transcription factor EGL-27 co-regulates DAF-16 target genes in response to DNA damage and together with DAF-16 promotes developmental growth. We propose that EGL-27/GATA activity specifies DAF-16 mediated DNA damage responses to enable developmental progression and to prolong tissue functioning when DNA damage persists.

Cells and tissues are constantly attacked by intrinsic and extrinsic genotoxic insults leading to a large variety of DNA lesions[1]. Congenital defects in genome maintenance systems underlie a variety of developmental abnormalities as well as cancer susceptibility and

[*]Correspondence: bjoern.schumacher@uni-koeln.de.
[6]present address: Centre for Integrative Physiology, University of Edinburgh, Edinburgh, EH8 9XD, United Kingdom
Author contributions: MM, LCR, VB, ME, RUM, AW, SG, JS performed experiments and analysed data; LCR, PF, BS conducted bioinformatics analysis; TB, BeS contributed materials; BS wrote the paper

The authors declare no competing financial interest.

Europe PMC Funders Author Manuscripts

progeroid ("premature aging-like") syndromes[2]. The two distinct damage recognition branches of nucleotide excision repair (NER) exemplify the complexity of phenotypes caused by genome maintenance defects. While global-genome (GG-) NER scans the entire genome, transcription-coupled (TC-) NER specifically recognizes lesions on the actively transcribed strand. In both cases the same downstream NER machinery removes the damage[3]. GG-NER defective patients develop the skin cancer susceptibility syndrome Xeroderma pigmentosum (XP), whereas TC-NER defective Cockayne syndrome (CS) patients exhibit severe postnatal growth failure followed by premature signs of aging. Mutations affecting the downstream NER components can lead to XP, XP in combination with CS (XPCS), trichothiodystrophy (TTD), or Cerebro-Oculo-Facio-Skeletal Syndrome (COFS)[3]. It is thought that GG-NER defects result in mutations and genome instability during replication and thus lead to cancer development, while RNA polymerase (RNAPII) stalling at DNA lesions as a result of TC-NER defects impairs developmental growth and accelerates degeneration of tissues[4].

Cellular DNA damage checkpoints that halt the cell cycle, or induce cellular senescence and apoptosis have been characterized over the past 25 years[5]. However, it remains poorly understood how DNA damage responses regulate organismal development and maintain tissue functionality when damage accumulates with aging. Given the complex disease phenotypes of genome instability syndromes it is of pivotal interest to uncover the mechanisms through which developing organisms and differentiated tissues respond to persistent DNA damage. *C. elegans* shows a clear distinction between highly dynamic germ cells undergoing mitotic and meiotic cell divisions and somatic cells that undergo a deterministic developmental fate until they terminally differentiate[6]. Highly conserved DNA damage checkpoint mechanisms respond to DNA damage specifically in the germ line[7]. The NER pathway is functionally conserved in the nematode[8]. Completely NER deficient *xpa-1* or *csb-1;xpc-1* double mutants are exquisitely UV sensitive. TC-NER defective *csb-1* but not GG-NER defective *xpc-1* mutant worms display UV sensitivity during late embryonic and early larval development. In contrast, UV irradiation of *xpc-1* but not *csb-1* mutants confer sterility during adulthood, and lethality in early embryos[9].

We have followed the larval development of *C. elegans* upon UV-induced DNA damage. While developmental growth transiently arrests, specifically somatic tissues cease developmental growth when transcription-blocking lesions remain unrepaired. We reveal that insulin/insulin-like growth factor signalling (IIS) -a conserved pathway regulating development, stress resistance, and lifespan[10]-responds to DNA damage. The IIS effector transcription factor DAF-16/FoxO is activated in response to persistent DNA damage in somatic tissues and, contrasting its established function in the starvation response, promotes developmental growth. The DNA damage responsiveness of DAF-16 is most effective during development and declines with aging. We propose that the growth promoting activity of DAF-16 is specified by the GATA transcription factor EGL-27, which we demonstrate to interact with DAF-16, co-regulates DAF-16 target genes and together with DAF-16 mediates DNA damage tolerance. Our data suggest that through GATA mediated promoter recognition DAF-16 activation enables development when DNA damage persists and

confers enhanced tissue functionality and lifespan amid DNA damage accumulation in aging.

Results

TC-NER deficiency leads to developmental arrest of somatic tissues upon UV damage

Upon hatching *C. elegans* successively undergoes the L1, L2, L3 and L4 larval stages preceding adulthood. In synchronized wild-type (wt) L1 larvae developmental growth was transiently delayed upon UVB treatment (Suppl. Figure 1A). While completely NER defective *xpa-1* mutants arrest larval development already at low UV doses (Suppl. Figure 1B), in UV-treated TC-NER deficient *csb-1* mutants germ cells continued their mitotic expansion while somatic development was impaired (Figure 1A). The germ cell proliferation was abrogated in *csb-1;xpc-1* double mutants similarly to *xpa-1* mutants, while GG-NER defective *xpc-1* mutants, despite completing somatic development, failed to develop a germ line upon UV treatment (Figure 1A). Mitotically dividing germ cells displayed anaphase bridges upon UV treatment of adult *xpc-1* mutants indicating genome instability in the germ stem cell compartment as the cause for sterility in GG-NER mutants (Suppl. Figure 1C). These data suggest that rather than functioning during different developmental periods as previously thought[9], already during larval development the two NER branches in *C. elegans* show specific requirements of GG-NER in germ cells and of TC-NER in somatic tissues.

Persistent DNA damage leads to activation of DAF-16/FoxO

To identify genes that respond to UV-induced DNA damage during development we analysed the transcriptomes of L1 larvae upon UV treatment. We verified microarray results using quantitative real time PCR (Suppl. Table 1). 6 hours after 60mJ/cm^2 UV irradiation, 1349 genes were differentially expressed in wt worms ($p<0.01$, fold change (FC)>+/-1.5) (Suppl. Table 2) and 1730 genes responded ($p<0.01$, FC>+/-1.5) in *xpa-1* mutants that were treated with a low dose of 10mJ/cm^2 (Suppl. Table 3). The UV-induced gene expression changes in wt and *xpa-1* mutants showed a highly significant positive correlation (Spearman $r=0.89$; $p<0.0001$), indicating that the transcriptional response depended on UV-induced DNA lesions (Suppl. Figure 1D, E).

To identify pathways that respond to DNA damage during development, we developed “wormpath”, an algorithm that provides a statistical framework to measure enriched genetic or biochemical interactions reported in the *C. elegans* repository[11] (see methods). The largest significantly overrepresented network among UV response genes was centred on the IIS genes *daf-16* and *daf-2* ($p<0.0001$; Figure 1B) and comprised significantly overrepresented biological processes that included dauer larval development, determination of adult lifespan, and aging (Suppl. Figure 1F), indicating that genes functioning in the IIS longevity assurance pathway respond to DNA damage during development.

The FoxO transcription factor DAF-16 is activated when inhibitory IIS is alleviated and hypophosphorylated DAF-16 localizes to the nucleus to regulate starvation responses, confer resistance to multiple stress factors and mediate lifespan extension[12-16]. To address whether

Europe PMC Funders Author Manuscripts

DAF-16 is activated by DNA damage, we monitored DAF-16::GFP localization *in vivo*[16]. While in the absence of UV DAF-16::GFP was completely cytoplasmic, we observed a transient nuclear localization upon UV treatment during larval stages (L1 larvae Figure 1C; L3 larvae Suppl. Figure 1G). DAF-16 showed nearly complete and prolonged nuclear localization in completely NER and TC-NER deficient mutants upon UV damage, while GG-NER defective worms behaved similarly to wt animals (Figure 1C; Suppl. Figure 1G), suggesting that transcription-blocking lesions lead to activation of DAF-16. The kinetics of DAF-16 translocation within several hours following UV exposure is indeed consistent with the kinetics of RNAPII dependent detection of transcription-blocking lesions[17].

During adulthood, we observed that DAF-16::GFP nuclear localization in response to DNA damage occurs most readily at day 3 and then declines as the worms age (Figure 1D). Also the strong DAF-16 activation in *xpa-1* mutants occurs during early adulthood and then steadily declines throughout adulthood (Figure 1D; Suppl. Figure 2A). The initial induction of CPD lesions by UV was unaffected by age (Suppl. Figure 2B, C). In contrast, DAF-16::GFP activation upon even mild heat stress remained constant throughout adulthood. These observations suggest that while DAF-16 activation occurs efficiently during larval development and in young adulthood, the DAF-16 responsiveness specifically to DNA damage declines with aging.

DAF-16 activation alleviates developmental arrest and enhances somatic tissue functionality when DNA damage persists

The function of DAF-16 in mediating lifespan extension and stress resistance has become evident through analysis of mutations in the insulin/IGF-1 receptor *daf-2* that lead to constitutive activation of DAF-16[14,15,18]. Complete loss-of-function of *daf-2* results in permanent L1 arrest[13] and strong loss-of-function alleles in permanent dauer arrest[19]. The canonical temperature sensitive *daf-2(e1370)* allele shows a slightly delayed but otherwise unperturbed development at the semi-permissive temperature of 20 °C (Figure 2, untreated)[18]. We also included mutants of *age-1*, the PI3 kinase acting downstream of DAF-2[20] and additional *daf-2* alleles (Figure 2; Suppl. Figure 2D). Strikingly, 48h post UV-treatment a significantly higher number of *daf-2* or *age-1* mutant animals had continued developmental growth while wt worms arrested (Figure 2). The alleviation of UV-induced arrest is the more striking as only mutants with partial loss of IIS function could be used for assessing developmental progress. *daf-2;daf-16* double mutants completely reconstituted UV-induced developmental arrest (Figure 2) comparable to wt or *daf-16* single mutants (Suppl. Figure 2E), demonstrating that DAF-16 activation is sufficient to promote developmental progression in response to UV-induced DNA damage. This role of activated DAF-16 to override the DNA damage-induced developmental arrest comprises a previously unknown function of DAF-16 that contrasts its role in starvation arrest, in which activated DAF-16 mediates the developmental stalling[13].

The alleviation of the developmental arrest upon DNA damage in *daf-2* mutants did not compromise adult longevity as subsequent adult lifespan was insignificantly reduced, whereas wt and *daf-2;daf-16* double mutants showed a slight but significant reduction of adult lifespan (Suppl. Figure 2F).

In contrast to DAF-16, the Nrf-related transcription factor SKN-1, functioning in parallel to DAF-16 to mediate lifespan extension and stress resistance[21,22], was dispensable for the DAF-16 mediated DNA damage tolerance during development (Suppl. Figures 3A-D).

To address whether DAF-16 activation might override the developmental arrest even when DNA damage persists, we UV-treated L1 worms that were defective in *daf-2* as well as in *xpa-1* precluding removal of UV-induced 6-4PP and CPD lesions (Figure 3A). Intriguingly, mutations in *daf-2* alleviated the arrest of *xpa-1* mutants in a *daf-16* dependent manner (Figure 3B) indicating that DAF-16 activation could override the developmental arrest despite the persistence of DNA lesions.

We then assessed whether the IIS response could also enhance functionality of differentiated tissues when DNA damage persists in adult worms and could thus antagonize DNA damage driven aging. In adult animals, UV damage leads to lifespan reduction in *xpa-1* mutant worms[23]. While *xpa-1* mutants showed a dramatic reduction in pharyngeal pumping and motility following UV treatment, the *xpa-1;daf-2* double mutants maintained tissue functionality (Figure 3C, D; Suppl. Figure 4A) and their lifespan was significantly extended compared to *xpa-1* mutants (Suppl. Figure 4B, C). Thus, *daf-2* inactivation enhances tissue functionality and healthy lifespan in the presence of persistent DNA damage.

To assess whether the enhanced resistance to persistent DNA damage and alleviation of developmental arrest of *daf-2* mutants comprised a specific function of DAF-16 in somatic tissues, we treated *csb-1;daf-2* and *xpc-1;daf-2* mutants. While *age-1* and *daf-2* mutations alleviated the arrest of *csb-1* mutants upon UV in a *daf-16* dependent manner (Figure 3E), mutant *daf-2* failed to confer UV-resistance to *xpc-1* deficient germ cells (Figure 3F). In addition, the DNA damage tolerance in *daf-2* mutants was unaffected in germline-less *glp-4* mutants (Suppl. Figure 4D). Thus, DAF-16 activation enhances tolerance of persistent DNA damage specifically in somatic tissues.

DAF-16 promotes developmental growth through distinct target gene regulation in response to DNA damage

To assess the role of DAF-16 in developmental gene regulation, we contrasted the gene expression changes upon UV treatment with those upon starvation, where DAF-16 has previously been shown to mediate L1 arrest[13]. In agreement with previous gene expression data[24], we observed a strong transcriptional response to starvation (Table S4). The significantly altered transcripts in response to UV and to starvation showed a highly significant positive correlation (Spearman $r=0.62$; $p<0.0001$) (Figure 4A, Suppl. Figure 1C) with 64% of UV response genes overlapping with the starvation response genes (Figure 4B). 82% of those overlapping genes responded similarly to UV as to starvation (Suppl. Tables 5, 6) and contained oxidative stress responses. The genes that were induced in response to UV and repressed in response to starvation showed enrichment of positive regulation of metazoan growth (Figure 4C, Suppl. Figure 5).

Systematic analysis of putative promoter elements employing the RSAT software[25] revealed a highly significant enrichment of the DAF-16 associated element (DAE)[26] within the UV-induced genes, while starvation induced genes showed highly significant enrichment of the

DAF-16 binding element (DBE) (Table 1). Most strikingly, those genes that were induced both upon UV and starvation showed overrepresentation of DBE, while those genes that were induced upon UV and repressed upon starvation contained a highly significant enrichment of DAE. None of the binding sites associated with the transcription factors PHA-4, DAF-12, ELT-2, HSF-1, SKN-1, or the canonical E-box showed such enrichment patterns, indicating a vastly specific enrichment of DAF-16 target promoters (Table 1, Suppl. Table 7, 8). This promoter analysis suggests that DAF-16 activation in response to UV-induced DNA damage leads to induction of DAE regulated genes, which are repressed by DAF-16 upon starvation. Indeed, starvation prior to UV exposure resulted in exacerbated developmental arrest (Figure 4D) suggesting that the induction of starvation responses sensitizes worms for developmental arrest following DNA damage. SKN-1, previously implied in the starvation response[27], was dispensable for this effect (Suppl. Figure 6A).

The GATA transcription factor EGL-27 interacts with DAF-16 to induce DNA damage response genes and promote developmental growth

To identify transcription factors that might specify the distinctive growth promoting function of DAF-16 in the DNA damage response, we determined DAF-16 dependent genes as being significantly induced (FC>1.5; p<0.01) upon UV in *daf-2* mutants and more strongly induced upon UV in *daf-2 vs. daf-2;daf-16*, *daf-2 vs. wt*, and *wt vs. daf-16* (Suppl. Table 9), yielding 514 genes, among which the largest group was indeed associated with positive regulation of growth (Suppl. Figure 6B, Suppl. Table 10). The DAF-16 dependent UV-response genes contained 3 significantly enriched sequence matrices that comprise GATA transcription factor recognition sites (Figure 5A), as determined by motif comparison analysis[28]. Two motifs contained the DAE element (CTTATCA or TGATAAG) that in addition to its identification as DAF-16 target element[29], has also been defined as GATA response element[30]. Indeed, several GATA factors are required for the longevity of *daf-2* mutants[30-32]. To investigate the function of GATA factors in the developmental response to UV irradiation, we analysed *elt-3*, *elt-4*, *elt-6*, *elt-7*, *egl-27*, *end-1*, *end-3*, *med-1*, and *med-2* mutants. Specifically *egl-27* mutants exhibited a strongly enhanced developmental growth arrest following UV treatment (Figure 5B, Suppl. Figure 6C, D)) that was rescued by transgenic expression of EGL-27::GFP (Figure 5B).

Out of 22 tested DAF-16 target genes 12 showed significantly diminished induction upon UV irradiation in *egl-27* mutants when compared to wt (Figure 6A), indicating that EGL-27 regulates a subset of DAF-16 dependent DNA damage response genes. Among those, RNAi against the “DNA damage effector downstream of DAF-16 and EGL-27” (*dde*) genes *dde-1* (F01D5.1) and *dde-2* (F01D5.2), as well as a mutation in *oac-32*, which we renamed *dde-3*, significantly enhanced developmental arrest upon UV treatment (Figure 6B).

We next determined that EGL-27 and DAF-16 genetically interact by synergistically promoting developmental growth (Figure 6C (untreated), Suppl. Table 11). A *daf-16* mutation further enhanced the UV sensitivity of *egl-27* mutants (Figure 6C). Moreover, EGL-27 was required for the DNA damage tolerance of *daf-2* mutants, as *daf-2;egl-27* double mutants showed a similar degree of developmental arrest as wt worms (Figure 6D). *egl-27* mutants showed enhanced sensitivity to oxidative damage (which among others also

imposes transcription blocking lesions[33]) that was further aggravated in *daf-16;egl-27* double mutants (Suppl. Figure 7A). In contrast to *daf-16*, however, *egl-27* was dispensable for heat stress resistance (Suppl. Figure 7B) and *daf-2*- mediated dauer formation (Suppl. Figure 7C).

Cytologically, DAF-16::GFP and EGL-27::GFP fusion proteins were expressed in the same nuclei in L1 animals following UV-treatment (Figure 7A, Suppl. Figure 7D). *In vitro*, co-expressed epitope tagged DAF-16 co-immunoprecipitated with EGL-27 (Figure 7B, Suppl. Figure 8A-E). We further mapped the interaction to the C-terminus containing a Q-rich domain (Suppl. Figure 8F) that is present in EGL-27 but not other *C. elegans* GATA factors (Figure 7B, Suppl. Figure 8A-E). Taken together, these data indicate that EGL-27 functions together with DAF-16 downstream of DAF-2 to specify the induction of developmental growth genes thus promoting tolerance to DNA damage.

Discussion

DAF-16 promotes development in response to DNA damage through distinct mode of gene regulation

We investigated the consequences of DNA damage during postembryonic metazoan development in *C. elegans* and determined that UV-induced DNA damage leads to a transient arrest during larval development. TC-NER defects specifically impair the development of somatic tissues, suggesting that the requirement for TC-NER for developmental growth is conserved from worm to man. Given the phenotypic complexity of mammalian NER mutants, we propose *C. elegans* as valuable metazoan system to gain insight into physiological consequences of DNA damage during development and aging particularly in the context of distinct NER impairments.

We reveal that an IIS network responds to UV-induced DNA damage in developing worms. Activation of the IIS effector DAF-16 was previously observed in response to various stressors including starvation, heat, and juglone but not UV[16]. In contrast to previous studies that used short wavelength UVC, which is unlikely to penetrate throughout the worm's tissues, we observed DAF-16 activation upon irradiation with more deeply penetrating and physiologically more relevant UVB. Natural sampling experiments identified developing *C. elegans* larvae outside of the starvation arrest exclusively on decaying fruits and fresh compost heaps[34]. With a yearly average irradiation in central Europe of 4mJ/cm^2 UVB per minute, with significantly higher peaks during summer and at higher altitudes[35], the UV response mechanisms are thus likely to play an important role in the natural habitat of *C. elegans*. In contrast to the transient activation in repair proficient animals, persistent DNA damage resulted in enhanced and prolonged DAF-16 activation. DAF-16 activation specifically in response to UV-treatment declined during adulthood, suggesting that reduced DAF-16 responsiveness to DNA damage accumulation contributes to DNA damage driven tissue degeneration with aging.

In accordance with our observations, reduced IIS has been observed in progeroid mice lacking Sirtuin 6[36], or the NER factors *Ercc1* or *Csb* and *Xpa*[37,38]. We previously showed that persistent DNA damage that leads to RNAPII stalling, the culprit of TC-NER

deficiencies, evokes IIS attenuation in mammalian cells[39]. We now for the first time reveal the physiological function of IIS response to persistent DNA damage. We show that genetic IIS attenuation leads to suppression of the DNA damage induced somatic growth arrest through activation of DAF-16. This previously unknown function contrasts the established role of DAF-16 in response to starvation[13]. In both cases DAF-16 confers general stress resistance as observed upon starvation, heat, reactive oxygen species, and UV[12,14,16,40,41] likely through the induction of DBE-controlled genes. Specifically in response to DNA damage, DAF-16 induces starvation-repressed growth genes that contain GATA-comprising DAE motifs (Figure 7C). Conceptually consistent with a dual function, the activation of the mammalian DAF-16 homolog also results in very contrasting consequences as FoxO acts tumour suppressive in solid tumours but oncogenic in an acute myeloid lymphoma[42]. It will be highly interesting to evaluate whether context-dependent transcription co-factors determine the distinct outcomes of FoxO activity.

ELG-27/GATA co-regulates developmental growth with DAF-16/FoxO

Our data suggest that DAF-16 induces developmental growth genes through binding to a C-terminal interaction domain of EGL-27 whose GATA domain in turn recognizes the GATA/DAE promoter motif. We genetically place EGL-27 downstream of DAF-2 in promoting developmental growth in parallel to DAF-16. *egl-27* has previously been found to regulate cell polarity, migration, and embryonic patterning redundantly with the related GATA factor *egr-1*[43-45]. The human EGL-27 homolog metastasis tumour antigen 1 (MTA1) is associated with aggressiveness of various tumour types[46,47] and is required for an efficient G2/M arrest following DNA damage[48]. It will be highly interesting to investigate whether FOXO and MTA1 interact in the DNA damage response and which implication this might have for tumour development and metastasis.

DAF-16 activation raises threshold for detrimental consequences of persistent DNA damage in development and aging

DAF-16 activity overrides the developmental arrest and enhances tissue functionality even in the absence of UV-lesion repair. DAF-16 activation might thus raise the threshold of damage-induced functional decline amid accumulating DNA damage with aging. Altering the tolerance threshold to persistent DNA damage through modifying IIS activity might comprise an evolutionary strategy to adapt the durability of somatic tissues without altering the DNA repair capacity, which would require adaptations in multiple genome maintenance systems and in case of NER involve multi-protein complexes with abundant base line levels that are assembled upon damage recognition with highly complex dynamics[49].

The function of DAF-16 in responding to DNA damage during development might be highly relevant also for understanding how longevity assurance pathways counteract the consequences of DNA damage accumulation in aging. As selective pressure acts most strongly during early life[50], IIS function might have been primarily adapted to respond to DNA damage during development. In *C. elegans* cellular DNA damage checkpoints are important for eliminating germ cells that are genomically compromised thus preventing resource allocation to damaged oocytes. Once embryogenesis ensues, cellular DNA damage checkpoints are switched off[7]. In the subsequent larval development the IIS response might

force growth even when DNA damage persists thus ensuring the maximal usage of previously invested maternal resources. Developmental timing and lifespan are intricately linked as slowly developing organisms require a longer lifespan for successful reproduction[51]. The IIS response to DNA damage might thus also adapt to co-regulate developmental timing and lifespan in response to persistent DNA damage.

Experimental Procedures

Strains

All strains were cultured according to standard conditions[54]. Strains used were N2 (Bristol; wild type), RB1801 *csb-1(ok2335)*, RB864 *xpa-1(ok698)*, FX03886 *xpc-1(tm3886)*, CB1370 *daf-2(e1370)*, DR1572 *daf-2(e1368)*, DR1565 *daf-2(m596)*, DR26 *daf-16(m26)*, TJ1052 *age-1(hx546)*, DR1309 *daf-2(e1370);daf-16(m26)*, TJ356 *zIs356[daf-16::GFP; rol-6]*IV, BJS10 *daf-2(e1370)*; *xpa-1(ok69 8)*, BJS27 *xpa-1(ok698)*; *age-1(hx546)*, BJS16; *zIs356[daf-16::GFP; rol-6]*IV; *xpa-1(ok698)*; BJS15 *zIs356[daf-16::GFP; rol-6]*IV; *csb-1(ok2335)*, BJS51: *xpc-1(tm3886); zIs356[daf-16::GFP; rol-6]IV*, BJS49: *csb-1(ok2335);xpc-1(tm3886); zIs356[daf-16::GFP; rol-6]IV*, BJS23 *csb-1(ok2335)*;*daf-2(e1370)*, BJS22 *csb-1(ok2335)*; *age-1(hx546)*, BJS25 *csb-1(ok2335)*; *daf-16(m26)*, BJS30 *csb-1(ok2335)*; *daf-16(m26)*; *daf-2(e1370)*, BJS29 *xpc-1(tm3886)*; *daf-2 (e1370)*, BJS21 *csb-1(ok2335)*; *xpc-1(tm3886)*, CF1934 daf-16(mu86)I;muIs109[daf-16p::gfp::daf-16 + odr-1p::rfp], MT170 *egl-27(n170)*, VC1217 *egl-27(ok1670)*, BJS143 *daf-2(e1370);egl27(ok1670)*, OP177 unc-119(ed3)III; wgIs177[egl-27::TY1::EGFP::3xFLAG + unc-119(+)], BJS151 egl-27(ok1670)II; unc-119(ed3)III; wgIs177[egl-27::TY1::EGFP::3xFLAG + unc-119(+)], BJS150 egl-27(n170)II; unc-119(ed3)III; wgIs177[egl-27::TY1::EGFP::3xFLAG + unc-119(+)], VC40566 *dde-3(gk696370)*, BJS267 *skn-1(zu169)nT1qIS51*, BJS268 *skn-1(zu67)nT1qIS51*, BJS263 *skn-1(zu135)nT1qIS51*, BJS264 *skn-1(zu135)nT1qIS51;daf-2(e1370)*, BJS265 *skn-1(zu135)nT1qIS51;daf-16(mu86)*, BJS266 *skn-1(zu135)nT1qIS51;daf-2(e1370);daf-16(mu86)*, Is007*skn-1b/c::GFP;rol-6*, BJS226 *skn-1b/c::GFP;rol-6;xpa-1(ok698)*, SS104 *glp-4(bn2)*, BJS234 *glp-4(bn2);daf-2 (e1370)*, *VC143 elt-3(gk121)*, JM124 *elt-4(ca16)*, VC1606 *elt-6(gk754)*, RB948 *elt-7(ok835)*, VC271 *end-1(ok558)*, RB1331 *end-3(ok1448)*, RB930 *med-1(ok804)*, MS123 *med-2(cx9744)*.

Microarrays

RNA was isolated from 10000 age synchronized L1 larvae. The worms were age synchronized using hypochlorite treatment. Since hypochlorite treatment is followed by hatching in media without food and thus induces a starvation response, after 24h of hatching the larvae were transferred to NGM plates seeded with *E. coli* OP50 bacteria and left to recover for 6h before UV treatment to remove any effect of starvation on their transcriptional profile. The starvation control was not transferred to seeded plates. 6h after treatment with the indicated doses of UVB radiation using a UV6 lamp (Waldmann), the animals were washed off plates using M9 buffer, washed once more with M9 buffer and resuspended in TRIZOL (Invitrogen). To facilitate complete lysis, worms were disrupted in TRIZOL with 0.7 mm zirconia/silica beads (Biospec Products) using a Precellys24 (Bertin). After lysis, total RNA was purified using the RNeasy Mini kit (Qiagen) according to the

Europe PMC Funders Author Manuscripts

manufacturers' specifications, except for the use of 1-Bromo-3-chloropropane (Sigma) instead of chloroform for phase separation.

RNA quality was assessed using a Nanodrop 8000 spectrophotometer (Thermo Scientific) and a Bioanalyzer (Agilent). Expression profiles were obtained using a GeneChip *C. elegans* Genome Array (Affymetrix) according to the manufacturers' specifications by the CCG facility (Berlin, Germany). Hybridization signals were normalized by quantile normalization and differentially expressed genes were determined by ANOVA analysis using the Partek software package.

The data files are deposited under the GEO accession code GSE47778.

For qPCR analysis, cDNA was generated using Superscript II (Invitrogen). Quantitative real-time PCR (qPCR) was done with Biorad CFX96 real-time PCR machines using SYBR Green I (Sigma) and Platinum Taq polymerase (Invitrogen). All qPCR reactions were done in duplicate. The generation of specific PCR products was confirmed by melting curve analysis. Each primer pair was tested with a logarithmic dilution of a cDNA mix to generate a linear standard curve (crossing point (CP) plotted versus *log* of template concentration), which was used to calculate the primer pair efficiency ($E = 10^{(-1/slope)}$). For data analysis, the second derivative maximum method was applied, and induction of target cDNA was calculated according to Pfaffl[55]: $[E_{target}{}^{\Delta CP(cDNAuntreated-cDNAtreated)target}]/[E_{control}{}^{\Delta CP(cDNAuntreated-cDNAtreated)control}]$.

Pathway analysis with a newly developed algorithm

For in-depth analysis of the content of our set of differentially expressed genes, we have developed *Wormpath*, a user-friendly software and web service for efficient discovery of genetic networks in *C. elegans* taking advantage of the information on genetic interactions available in *Wormbase*. A single "interaction" between two genes can describe their role as members of the same pathway; moreover, a set of interactions can be understood as components of large networks as a model for complex cellular processes or signalling cascades. For reasons of stringency we have only included experimentally verified interactions in *Wormbase*, while ignoring predicted interactions. *Wormpath* uses pairs termed "indirect" interactions, which are interactions between two genes from the list of significant genes and a third gene, which is not in the list. This strategy allows the identification of interaction networks also when, for instance, only some genes functioning in a pathway are transcriptionally altered while other members of a pathway might also be regulated e.g. on the posttranscriptional level.

The search algorithm operates on a large underlying graph in which each gene of the list is assigned exactly one node. Pairs of nodes in the graph linked by a direct or "indirect" genetic interaction according to *Wormbase* are assigned an edge labelled with additional information from the database. Our approach for discovery of networks in this graph is controlled by a maximum number of steps *D* defining the distance from a start node, of which interacting nodes are searched. This strategy is applied to each of the nodes in the graph taken as the start node and, subsequently, all redundant networks are discarded. To also analyse smaller sub-networks, the procedure is repeated for all possible step sizes

smaller than *D* because this number naturally controls the degree of completeness to which a particular network is made visible.

To rank the networks in the results list, each of them is assigned a score defined by the number of its interactions, thus reflecting its size as well as its complexity. A *p*-value indicating the statistical significance of the test on the null hypothesis that the proportion of pathway members is equal among the list members and in the entirety of all *C. elegans* genes is calculated by Fisher's exact test with the hypergeometric parameters *N* (total number of genes in the database), *n* (number of differentially expressed genes) and *K* (total number of genes involved in the pathway estimated by the sum of the numbers of interactors of the pathway members among the differentially expressed genes). The software is accessible http://bifacility.uni-koeln.de/wormpath using a standard web browser.

Gene Ontology Classification and Overrepresentation of Biological Themes

All significant gene entries were subjected to GO classification (http://www.geneontology.org). Significant over-representation of GO-classified biological processes was assessed by comparing the number of pertinent genes in a given biological process to the total number of the relevant genes printed on the array for that particular biological process (Fisher exact test) using the publicly accessible software DAVID (http://david.abcc.ncifcrf.gov/summary.jsp). Due to the redundant nature of GO annotations, we employed Kappa statistics to measure the degree of the common genes between two annotations, and heuristic clustering to classify the groups of similar annotations according to kappa values (http://david.abcc.ncifcrf.gov/summary.jsp).

Transcription factor sites analysis

Only genes with a p-value<0.01 were considered for the clustering of responsive transcripts to UV or/and starvation. We clustered the genes in upregulated (1.5 or 2 fold change for UV and starvation response, respectively) and downregulated response (−1.5 and −2 fold change for UV and starvation response, respectively). Three analyses of the promoter regions of the genes were performed with these data: first a search with the sequences included in both responses separately, second with the non-overlapped responses and, finally, with the overlapped ones. We searched either 600 or 1000 base pairs upstream of the start codon, for TGTTTAC the canonical DAF-16 Binding Element (DBE) motif[56]; CTTATCA the predicted DAF-16 Associated Element (DAE)[26]; NTTCNNGAANNTTCN, NTTCNNGAAN$(N)_5$NGAAN and NTTCN$(N)_5$NTTCN$(N)_5$NGAAN the Heat Shock Elements (HSE)[57]; WWTRTCAT the SKN-1 binding motif[22] and CATATG an Heme-responsive element[58]. Transcription factor sites search was performed using the DNA-pattern matching tool of regulatory sequence analysis tools RSAT software (http://rsat.ulb.ac.be/rsat/)[25]. The results given are the total percentage of matches for each cluster, in both strands of the sequence. The *p*-values were obtained with the 2-tailed Fisher's exact test, in respect to all the corresponding *C. elegans* sequences of genes that did not significantly respond to either UV or starvation.

In order to search for overrepresented motifs in the promoter regions of the DAF-16 dependently induced genes, 1000 bp upstream the CDS of 449 genes that were significantly

induced in *daf-2* (FC>1.5; p<0.01) upon UV and more strongly induced upon DNA damage in *daf-2 vs. daf-2;daf-16*, *daf-2 vs. wt*, and *wt vs. daf-16* were submitted to the oligo-analysis tool in RSAT. The search was limited to sequence alignments of seven nucleotides. We validated the significance of the motifs by reassessing the percentage of sequences containing the motifs in the group of genes and by comparing this percentage with promoter of all genes that did not alter their expression upon UV treatment. We used TOMTOM, a Motif Comparison Tool, to search similarities between the motifs found in the group of interest and Transcription Factors databases. Employing the consensus matrices sequences as input we obtained statistically significant motifs that were associated to TF of different species.

Irradiation and analysis of somatic arrest

Worms were bleached and allowed to hatch over night in M9 buffer. Arrested L1 larvae were put onto empty NGM plates and irradiated with 310nm UVB light using Phillips UV6 bulbs in a Waldmann UV236B irradiation device or were mock treated. (Irradiance was measured using a UVX digital radiometer and a UVX-31 probe from UVP and was generally around 0.3 mW/cm^2.) Worms were washed off with M9 buffer, concentrated by centrifugation and put on NGM plates with pre-grown OP50 *E.coli* lawn. Plates were kept at 20°C for 48hours or 72 hours, respectively, and analyzed by large particle flow cytometry using a Union Biometrica COPAS Biosort system. Larval stages were attributed by measuring concerning Time of Flight versus Extinction using the Biosort 5291 software and confirmed by manual inspection under a dissecting microscope.

Fecundity

Worms were staged and L4 larvae were irradiated and allowed to recover for 24 hours at 20°C. Worms were transferred to new OP50 seeded plates and allowed to lay eggs for 3 hours. Adult worms were removed and embryos counted. Viable offspring was counted 48h later.

DAF-16::GFP translocation

Strains TJ356: N2; *zIs356[daf-16::GFP; rol-6]IV*, BJS16: *xpa-1(ok698)I*; *zIs356[daf-16::GFP; rol-6]IV*, BJS15: *csb-1(ok2335)X*; *zIs356[daf-16::GFP; rol-6]IV*, BJS51: *xpc-1(tm3886); zIs356[daf-16::GFP; rol-6]IV* and BJS49: *csb-1(ok2335);xpc-1(tm3886); zIs356[daf-16::GFP; rol-6]IV*. DAF-16::GFP localization was analyzed under the fluorescence dissecting microscope at given time points. DAF-16::GFP localization of mock treated worms was invariably cytoplasmic throughout the experiments.

Pharyngeal pumping

Worms were synchronized by hypochlorite bleaching and L1s were put onto NGM plates seeded with OP50. After two days L4 larvae were transferred to new plates and 24 hours later were irradiated or mock treated. The worms were transferred every day to a new plate and on day 7 after irradiation the pharyngeal pumping rate of each healthy, surviving individual (at least 21 per strain and treatment) was determined under a dissecting stereo

microscope. To establish the average pharyngeal pumping rate, the movements of the pharynx of each individual were counted at least twice for 10 seconds and an average of these measurements was calculated. Box-and-whisker graph with Tukey whiskers of 1.5x IQR was created in Prism5 software.

Body bends

Worms were synchronized by hypochlorite bleaching and L1s were put onto NGM plates seeded with OP50. After two days L4 larvae were transferred to new plates and 24 hours later were irradiated or mock treated. The worms were transferred every day to a new plate and the rate of body bends was monitored on day 8 after irradiation. Each healthy, surviving individual (at least 18 per strain and treatment) was transferred into a drop of M9 buffer on a microscope slide, and body bends were monitored dissecting stereo microscope during periods of constant sigmoid movement (if possible). A body bend was scored each time the tip of the head reached the maximum amplitude on one given side. To establish the avarage body bend rate, the movements of each individual were counted at least 3 times for 10 seconds and an average of these measurements was calculated. Box-and-whisker graph with Tukey whiskers of 1.5x IQR was created on Prism5 software.

Lifespan

Adult worms were allowed to lay eggs for one hour and were removed. Progeny was incubated at 20°C and young adult worms were transferred to a new plate and irradiated with UVB or mock treated. Animals were incubated at 20°C and transferred to a new plate with a lawn of UV-sterilized OP50 bacteria every second day during the fertile period and once per week afterwards. Animals were counted every day or every second day. Dead animals were those that did not show any reaction after being poked with a platinum wire. Dead animals were scored and removed from the plate. Animals that died from internal hatching or dried out on the wall were censored.

DNA repair assay

Worms were grown on extra peptone plates, bleached and allowed to hatch over night in M9 buffer and filtered through a 11μm mesh filter (Millipore). Worms were pelleted and 100-200μl of worm pellet were transferred on to a medium NGM agar plates, left for drying and irradiated or mock treated. Worms were washed off immediately using pre-cooled M9 buffer, split into 2 parts and both parts were pelleted in a pre-cooled centrifuge. Supernatant was removed and one part was quick frozen on dry ice (0 minutes sample). The second sample was plated on a pre-seeded NGM plate and left on 20°C for about 22 hours. Worms were washed off using M9 buffer and washed 5 times, left rotating for 1-2 hours in M9 buffer in order to consume bacteria in the gut, washed 5 times, pelleted and quick frozen 24 hours after irradiation. Genomic DNA was isolated using Qiagen Puregene kit according to a modified version of the “DNA purification from Tissue” protocol. The frozen worm pellet was thawed at 4°C and 3ml of cell lysis solution and 15μl Proteinase K was added and the mix was incubated for 3hs at 55°C on a thermo shaker at full speed. Samples were allowed to cool down and 15μl of RNAse A solution was added and incubated for 30min at 37°C. Samples were cooled for 3min on ice and 1ml of protein precipitation solution was added and samples were vortexed vigorously for 20sec and centrifuged for 10min at 2,000 × g. The

supernatant was transferred to a new tube and 3ml of isopropanol were added and tubes were gently inverted 50 times. Samples were centrifuged for 3min at 2,000 × g and supernatant was removed and the pellet was allowed to air dry for 10min at RT. Genomic DNA was solved in 100µl Quiagen DNA rehydration buffer and DNA concentration was measured using a Nanodrop 8000 and DNA integrity was tested in on a 0.7% TAE gel. A 1:1 dilution series starting with 4µg for 6-4PPs and 1µg for CPDs and 7 dilution steps was carried out and dilutions were denatured for 5 minutes at 95C, put directly on ice, and blotted onto an Hybond nylon membrane (Amersham) using a Whatman 96-well slot blotting device at 300mbar vacuum. Cross-linking of the DNA was carried out for 2 hours at 80°C. The membrane was blocked for 30 minutes in 3% milk/PBS. Primary antibodies Anti-Cyclobutane Pyrimidine Dimers - Clone: TDM-2 or Anti-(6-4) photoproducts - Clone: 64M-2 - both mouse (Cosmo Bio) were diluted 1:10,000 or 1:3,000, respectively in PBS-T. The membrane was incubated in antibody solution over night at 4C, washed 3x in PBS-T, blocked for 30 minutes in 3% milk/PBS and incubated 1 hour with 1:10,000 secondary antibody solution Peroxidase-conjugated AffiniPure Goat Anti-Mouse IgG + IgM [H+L] (Jackson Immuno Research) in PBS-T at room temperature and washed 3x in PBS-T. DNA Lesions were visualized by incubating the membrane with ECL plus Western blotting reagent (Amersham) for 5min (0.1ml/cm2 of solution A and B 40:1) and exposing CL-Xposure Film (Thermo Scientific) to the membrane.

Heat shock

L4 worms were isolated onto NGM plates and incubated at 35°C until the time point indicated. Plates were removed and worms were allowed to recover for 30 minutes at 20°C and were analysed under a stereomicroscope. Worms were scored as dead when they did not respond to a poke with a platinum wire.

Dauer formation

Dauer formation rate was analysed by putting synchronized L1 worms derived from hypochlorite bleaching onto NGM plates seeded with OP50 and these plates were put to 25°C for 48hs. Worms were analysed for larval stage by inspection under a stereomicroscope.

Paraquat stress

Development on paraquat plates was analysed by putting synchronized L1 worms derived from hypochlorite bleaching onto NGM plates containing the indicated molarity of Methyl viologen dichloride hydrate (Paraquat 856177 Aldrich) seeded with OP50. Worms were scored 48hs later for their developmental stage.

Imaging of DAF-16::GFP and EGL-27::GFP transgenic animals

Imaging of live non-treated and UV-irradiated DAF-16 and EGL-27 reporter worms was done by laser scanning confocal microscopy using a Zeiss Meta 510. Synchronized L1 worms derived from hypochlorite bleaching were plated onto NGM plates seeded with OP50 and incubated at 20°C. Treated worms were irradiated with 150mJ/cm^2 UVB. Worms

were imaged 6hs after feeding and irradiation to visualize the cellular localization of the GFP fusion proteins.

In vitro interactions

daf-16 and *egl-27* cDNAs were cloned between the *MluI* and *NotI* sites in the mammalian expression vector pcDNA6, which contained FLAG or v5 in the C-terminus. Cloning primers DAF-16h: daf-16fwd AAAAACacgcgtgccaccATGcaactcgagcaaaagtcttca, daf-16rev AAAAACGCGGCCGCCcaaatcaaaatgaatatgctgccc; Cloning primers EGL-27d: *egl*-27fwd AAAAACacgcgtgccaccATGGCTGAATGTTCAGTAGGTGA, egl-27c-termfwd AAAAACACGCGTgccaccATGAGCGAGACTCCAGATCGT; egl-27rev AAAAACGCGGCCGCCCTGATGTTGAGGACGCATC, egl-27N-termrev AAAAACGCGGCCGCGCGAAGAAGGCGTTCTTCTTCGT. For Co-immunoprecipitation HEK293T cells were cultured in DME medium containing 10% FBS and transiently transfected using the calcium phosphate method. The following day, cells were harvested using ice-cold PBS. Cells were collected by centrifugation and lysed in a 1% Triton X-100 buffer (1% Triton X-100, 20 mM Tris-HCl, pH 7.5, 50 mM NaCl, 50 mM NaF, 15 mM $Na_4P_2O_7$, 2 mM Na_3VO_4 and PMSF) for 15 min on ice. After centrifugation at 15,000 *g* for 15 min at 4°C, the supernatant was incubated at 4°C for 2 h with anti-FLAG (M2) antibody coupled agarose beads (Sigma-Aldrich). Before the addition of beads, a small aliquot of each supernatant was preserved and diluted with 2× SDS-PAGE sample buffer for later Western blot analysis (lysate). The beads were washed at least three times with lysis buffer, and the proteins bound were resolved by SDS-PAGE, blotted on to polyvinylidene fluoride membranes, and visualized with enhanced chemiluminescence after incubation of the blots with the respective antibodies. Primary antibodies used were anti-FLAG (M2 Sigma-Aldrich), anti-V5 (SV5-Pk1 Serotec) and anti-GFP (Santa Cruz Biotechnology). Secondary antibodies coupled to horseradish peroxidase were obtained from Jackson ImmunoResearch Laboratories (goat anti-mouse IgG, light-chain specific) and DAKO (goat anti-mouse IgG). A truncation of hEPS15L1 [1-225] was used as a negative control[59].

Statistical analysis

Statistical methods that were used and error bar descriptions are detailed in the figure legends and specified for specific methodologies in the respective method section. Information about sample size is included in all figure legends. Randomization was not applied because the group allocation was guided by the genotype of the respective mutant worms. Worms of a given genotype were randomly selected from large strain populations for each experiment without any preconditioning. Blinding was not applied as the experiments were carried out under highly standardized and predefined conditions such that an investigator-induced bias can be excluded. Logrank-Test: The survival curves for the treatment conditions do not cross each other at any time point. t-Test: The variance within each group of data has been incorporated into the test statistics.

Supplementary Material

Refer to Web version on PubMed Central for supplementary material.

Europe PMC Funders Author Manuscripts

Europe PMC Funders Author Manuscripts

Acknowledgments

We thank S. Keller and K. Riehl for excellent technical assistance, D. Magner and A. Steckelberg for contributions earlier in the project, C. Jüngst and A. Schauss of the CECAD Imaging Facility, and J. Altmüller, I. Bässmann, and C. Becker of the CCG. Some strains were kindly provided by the Mitani lab and CGC (funded by the NIH Office of Research Infrastructure Programs (P40 OD010440)). VB received an IGSDHD, ME the EMBO long-term fellowship. BeS was supported by the Deutsche Forschungsgemeinschaft (SFB832 and SCHE 1562/2). BS acknowledges funding from the Deutsche Forschungsgemeinschaft (CECAD, SFB 829, SFB 670, and KFO 286), the European Research Council (ERC Starting grant 260383), Marie Curie (FP7 ITN CodeAge 316354, aDDRess 316390, MARRIAGE 316964, and ERG 239330), the German-Israeli Foundation (GIF, 2213-1935.13/2008 and 1104-68.11/2010), the Deutsche Krebshilfe (109453), and the BMBF (SyBaCol).

References

1. Loeb LA, Harris CC. Advances in chemical carcinogenesis: a historical review and prospective. Cancer Res. 2008; 68:6863–6872. [PubMed: 18757397]
2. Schumacher B, Garinis GA, Hoeijmakers JHJ. Age to survive: DNA damage and aging. Trends Genet. 2008; 24:77–85. [PubMed: 18192065]
3. Cleaver JE, Lam ET, Revet I. Disorders of nucleotide excision repair: the genetic and molecular basis of heterogeneity. Nat Rev Genet. 2009; 10:756–768. [PubMed: 19809470]
4. Wolters S, Schumacher B. Genome maintenance and transcription integrity in aging and disease. Front Genet. 2013; 4:19. [PubMed: 23443494]
5. Bartek J, Lukas J. DNA damage checkpoints: from initiation to recovery or adaptation. Curr. Opin. Cell Biol. 2007; 19:238–245. [PubMed: 17303408]
6. Sulston JE, Horvitz HR. Post-embryonic cell lineages of the nematode, Caenorhabditis elegans. Developmental biology. 1977; 56:110–156. [PubMed: 838129]
7. Gartner A, Milstein S, Ahmed S, Hodgkin J, Hengartner MO. A conserved checkpoint pathway mediates DNA damage--induced apoptosis and cell cycle arrest in C. elegans. Mol. Cell. 2000; 5:435–443. [PubMed: 10882129]
8. Stergiou L, Doukoumetzidis K, Sendoel A, Hengartner MO. The nucleotide excision repair pathway is required for UV-C-induced apoptosis in Caenorhabditis elegans. Cell Death Differ. 2007; 14:1129–1138. [PubMed: 17347667]
9. Lans H, et al. Involvement of global genome repair, transcription coupled repair, and chromatin remodeling in UV DNA damage response changes during development. PLoS Genet. 2010; 6:e1000941. [PubMed: 20463888]
10. Guarente L, Kenyon C. Genetic pathways that regulate ageing in model organisms. Nature. 2000; 408:255–262. [PubMed: 11089983]
11. Chen N, et al. WormBase: a comprehensive data resource for Caenorhabditis biology and genomics. Nucleic Acids Res. 2005; 33:D383–D389. [PubMed: 15608221]
12. Murakami S, Johnson TE. A genetic pathway conferring life extension and resistance to UV stress in Caenorhabditis elegans. Genetics. 1996; 143:1207–1218. [PubMed: 8807294]
13. Baugh LR, Sternberg PW. DAF-16/FOXO regulates transcription of cki-1/Cip/Kip and repression of lin-4 during C. elegans L1 arrest. Curr. Biol. 2006; 16:780–785. [PubMed: 16631585]
14. Ogg S, et al. The Fork head transcription factor DAF-16 transduces insulin-like metabolic and longevity signals in C. elegans. Nature. 1997; 389:994–999. [PubMed: 9353126]
15. Libina N, Berman JR, Kenyon C. Tissue-specific activities of C. elegans DAF-16 in the regulation of lifespan. Cell. 2003; 115:489–502. [PubMed: 14622602]
16. Henderson ST, Johnson TE. daf-16 integrates developmental and environmental inputs to mediate aging in the nematode Caenorhabditis elegans. Curr. Biol. 2001; 11:1975–1980. [PubMed: 11747825]
17. Riou L, et al. Differential repair of the two major UV-induced photolesions in trichothiodystrophy fibroblasts. Cancer Res. 2004; 64:889–894. [PubMed: 14871817]
18. Kenyon C, Chang J, Gensch E, Rudner A, Tabtiang R. A C. elegans mutant that lives twice as long as wild type. Nature. 1993; 366:461–464. [PubMed: 8247153]

19. Gottlieb S, Ruvkun G. daf-2, daf-16 and daf-23: genetically interacting genes controlling Dauer formation in Caenorhabditis elegans. Genetics. 1994; 137:107–120. [PubMed: 8056303]
20. Morris JZ, Tissenbaum HA, Ruvkun G. A phosphatidylinositol-3-OH kinase family member regulating longevity and diapause in Caenorhabditis elegans. Nature. 1996; 382:536–539. [PubMed: 8700226]
21. Tullet JMA, et al. Direct inhibition of the longevity-promoting factor SKN-1 by insulin-like signaling in C. elegans. Cell. 2008; 132:1025–1038. [PubMed: 18358814]
22. An JH, Blackwell TK. SKN-1 links C. elegans mesendodermal specification to a conserved oxidative stress response. Genes Dev. 2003; 17:1882–1893. [PubMed: 12869585]
23. Boyd WA, et al. Nucleotide excision repair genes are expressed at low levels and are not detectably inducible in Caenorhabditis elegans somatic tissues, but their function is required for normal adult life after UVC exposure. Mutat. Res. 2010; 683:57–67. [PubMed: 19879883]
24. Baugh LR, Demodena J, Sternberg PW. RNA Pol II accumulates at promoters of growth genes during developmental arrest. Science. 2009; 324:92–94. [PubMed: 19251593]
25. Thomas-Chollier M, et al. RSAT: regulatory sequence analysis tools. Nucleic Acids Res. 2008; 36:W119–27. [PubMed: 18495751]
26. Murphy CT, et al. Genes that act downstream of DAF-16 to influence the lifespan of Caenorhabditis elegans. Nature. 2003; 424:277–283. [PubMed: 12845331]
27. Paek J, et al. Mitochondrial SKN-1/Nrf mediates a conserved starvation response. Cell Metab. 2012; 16:526–537. [PubMed: 23040073]
28. Gupta S, Stamatoyannopoulos JA, Bailey TL, Noble WS. Quantifying similarity between motifs. Genome Biol. 2007; 8:R24. [PubMed: 17324271]
29. Curran SP, Wu X, Riedel CG, Ruvkun G. A soma-to-germline transformation in long-lived Caenorhabditis elegans mutants. Nature. 2009; 459:1079–1084. [PubMed: 19506556]
30. Budovskaya YV, et al. An elt-3/elt-5/elt-6 GATA transcription circuit guides aging in C. elegans. Cell. 2008; 134:291–303. [PubMed: 18662544]
31. Zhang P, Judy M, Lee S-J, Kenyon C. Direct and Indirect Gene Regulation by a Life-Extending FOXO Protein in C. elegans: Roles for GATA Factors and Lipid Gene Regulators. Cell Metab. 2013; 17:85–100. [PubMed: 23312285]
32. Xu X, Kim SK. The GATA Transcription Factor egl-27 Delays Aging by Promoting Stress Resistance in Caenorhabditis elegans. PLoS Genet. 2012; 8:e1003108. [PubMed: 23271974]
33. Charlet-Berguerand N, et al. RNA polymerase II bypass of oxidative DNA damage is regulated by transcription elongation factors. EMBO J. 2006; 25:5481–5491. [PubMed: 17110932]
34. Barriere A, Felix MA. Temporal dynamics and linkage disequilibrium in natural Caenorhabditis elegans populations. Genetics. 2007; 176:999–1011. [PubMed: 17409084]
35. Hader, DP.; Lebert, M. Environmental UV radiation: impact on ecosystems and human health and predictive models. Ghetti, F.; Checcucci, G.; Bornman, JF., editors. Vol. 57. Springer; 2006. p. 95-108.
36. Mostoslavsky R, et al. Genomic instability and aging-like phenotype in the absence of mammalian SIRT6. Cell. 2006; 124:315–329. [PubMed: 16439206]
37. Niedernhofer LJ, et al. A new progeroid syndrome reveals that genotoxic stress suppresses the somatotroph axis. Nature. 2006; 444:1038–1043. [PubMed: 17183314]
38. van der Pluijm I, et al. Impaired genome maintenance suppresses the growth hormone--insulin-like growth factor 1 axis in mice with Cockayne syndrome. PLoS Biol. 2006; 5:e2. [PubMed: 17326724]
39. Garinis GA, et al. Persistent transcription-blocking DNA lesions trigger somatic growth attenuation associated with longevity. Nat. Cell Biol. 2009; 11:604–615. [PubMed: 19363488]
40. Hsu AL, Murphy CT, Kenyon C. Regulation of aging and age-related disease by DAF-16 and heat-shock factor. Science. 2003; 300:1142–1145. [PubMed: 12750521]
41. Johnson TE, et al. Longevity genes in the nematode Caenorhabditis elegans also mediate increased resistance to stress and prevent disease. J Inherit Metab Dis. 2002; 25:197–206. [PubMed: 12137228]

42. Sykes SM, et al. AKT/FOXO Signaling Enforces Reversible Differentiation Blockade in Myeloid Leukemias. Cell. 2011; 146:697–708. [PubMed: 21884932]
43. Solari F, Bateman A, Ahringer J. The Caenorhabditis elegans genes egl-27 and egr-1 are similar to MTA1, a member of a chromatin regulatory complex, and are redundantly required for embryonic patterning. Development. 1999; 126:2483–2494. [PubMed: 10226007]
44. Ch'ng Q, Kenyon C. egl-27 generates anteroposterior patterns of cell fusion in C. elegans by regulating Hox gene expression and Hox protein function. Development. 1999; 126:3303–3312. [PubMed: 10393110]
45. Herman MA, et al. EGL-27 is similar to a metastasis-associated factor and controls cell polarity and cell migration in C. elegans. Development. 1999; 126:1055–1064. [PubMed: 9927605]
46. Kumar R, Wang RA, Bagheri-Yarmand R. Emerging roles of MTA family members in human cancers. Semin Oncol. 2003; 30:30–37. [PubMed: 14613024]
47. Nicolson GL, et al. Tumor metastasis-associated human MTA1 gene and its MTA1 protein product: role in epithelial cancer cell invasion, proliferation and nuclear regulation. Clin Exp Metastasis. 2003; 20:19–24. [PubMed: 12650603]
48. Li DQ, Ohshiro K, Khan MN, Kumar R. Requirement of MTA1 in ATR-mediated DNA damage checkpoint function. J Biol Chem. 2010; 285:19802–19812. [PubMed: 20427275]
49. Luijsterburg MS, et al. Stochastic and reversible assembly of a multiprotein DNA repair complex ensures accurate target site recognition and efficient repair. The Journal of Cell Biology. 2010; 189:445–463. [PubMed: 20439997]
50. Kirkwood TB. Understanding the odd science of aging. Cell. 2005; 120:437–447. [PubMed: 15734677]
51. de Magalhaes JP, Church GM. Genomes optimize reproduction: aging as a consequence of the developmental program. Physiology (Bethesda). 2005; 20:252–259. [PubMed: 16024513]
52. Kamath RS, et al. Systematic functional analysis of the Caenorhabditis elegans genome using RNAi. Nature. 2003; 421:231–237. [PubMed: 12529635]
53. Reboul J, et al. C. elegans ORFeome version 1.1: experimental verification of the genome annotation and resource for proteome-scale protein expression. Nat. Genet. 2003; 34:35–41. [PubMed: 12679813]

Additional References

54. Brenner S. The genetics of Caenorhabditis elegans. Genetics. 1974; 77:71–94. [PubMed: 4366476]
55. Pfaffl MW. A new mathematical model for relative quantification in real-time RT-PCR. Nucleic Acids Res. 2001; 29:e45. [PubMed: 11328886]
56. Furuyama T, Nakazawa T, Nakano I, Mori N. Identification of the differential distribution patterns of mRNAs and consensus binding sequences for mouse DAF-16 homologues. Biochem. J. 2000; 349:629–634. [PubMed: 10880363]
57. Sakurai H, Enoki Y. Novel aspects of heat shock factors: DNA recognition, chromatin modulation and gene expression. FEBS J. 2010; 277:4140–4149. [PubMed: 20945530]
58. Sinclair J, Hamza I. A novel heme-responsive element mediates transcriptional regulation in Caenorhabditis elegans. J Biol Chem. 2010; 285:39536–39543. [PubMed: 20938051]
59. Habbig S, et al. NPHP4, a cilia-associated protein, negatively regulates the Hippo pathway. The Journal of Cell Biology. 2011; 193:633–642. [PubMed: 21555462]

Europe PMC Funders Author Manuscripts

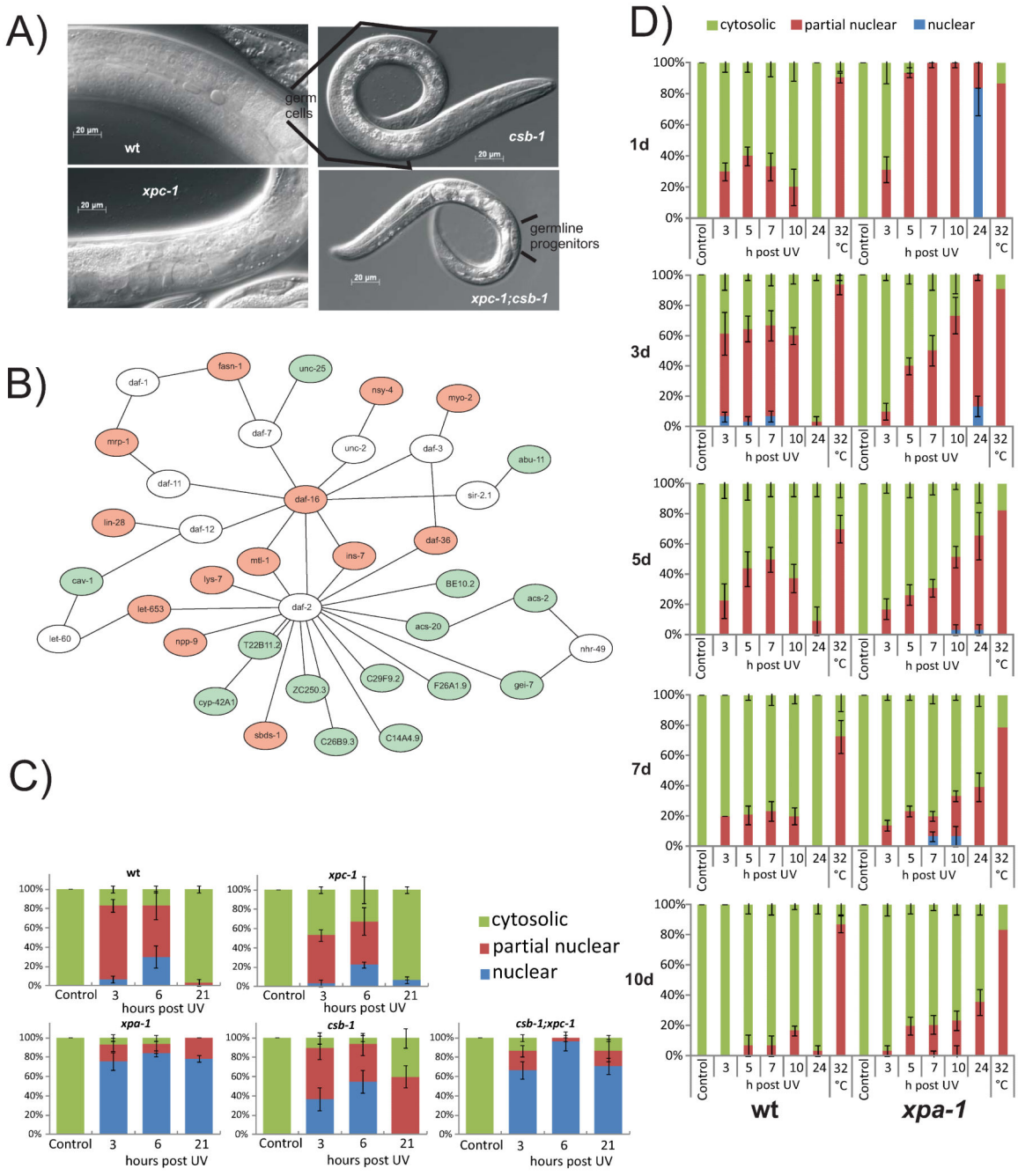

Figure 1. IIS network responds to UV-induced DNA damage during development and activation of DAF-16 that declines with aging

(A) Transcription-coupled repair defects lead to arrested somatic development. Worms were treated as L1 larvae and pictures taken 96h post treatment (wt, *xpc-1*, *csb-1* with 60mJ/cm^2; *xpc-1;csb-1* with 10mJ/cm^2). Note that while wt worms have developed into adult worms, *xpc-1* mutants have completed somatic development but lack a germ line, c*sb-1* mutants are developmentally delayed while germ cells continued to divide while *xpc-1;csb-1* double mutants have arrested both somatic and germ line development (representative pictures shown, experiment was repeated at least 3 times). (B) shows largest significantly

Europe PMC Funders Author Manuscripts

overrepresented interaction network among differentially expressed genes upon UV treatment. Upregulated genes are depicted in red, downregulated genes in green. One link through non-transcriptionally regulated genes was permitted in the analysis. (C) DAF-16::GFP cellular localization upon UV treatment in larvae. L1 wt, *xpc-1*, *xpa-1*, *csb-1* and *csb-1;xpc-1* strains were irradiated with 120 mJ/cm^2 and kept at 20°C (Average of n=3 independent experiments per strain and dose is shown, 10 individuals analysed per experiment; error bars=SEM). The graph shows the percentage of worms showing cytoplasmic, nuclear and partially nuclear DAF-16::GFP localization without treatment (control), and following UV irradiation. (D) DAF-16::GFP cellular localization upon UV treatment in adult worms. Wt and *xpa-1* mutant are shown. Three replicates of 10 adult worms during the first, third, fifth, seventh and tenth day of adulthood were exposed to 150 mJ/cm^2 and incubated at 20°C. In parallel, adult worms of the same age were heat shocked at 32°C for ten minutes and scored for the subcellular localization of the GFP signal (Average of n=3 independent experiments per strain and dose is shown, 10 individuals analysed per experiment; error bars=SEM).

Europe PMC Funders Author Manuscripts

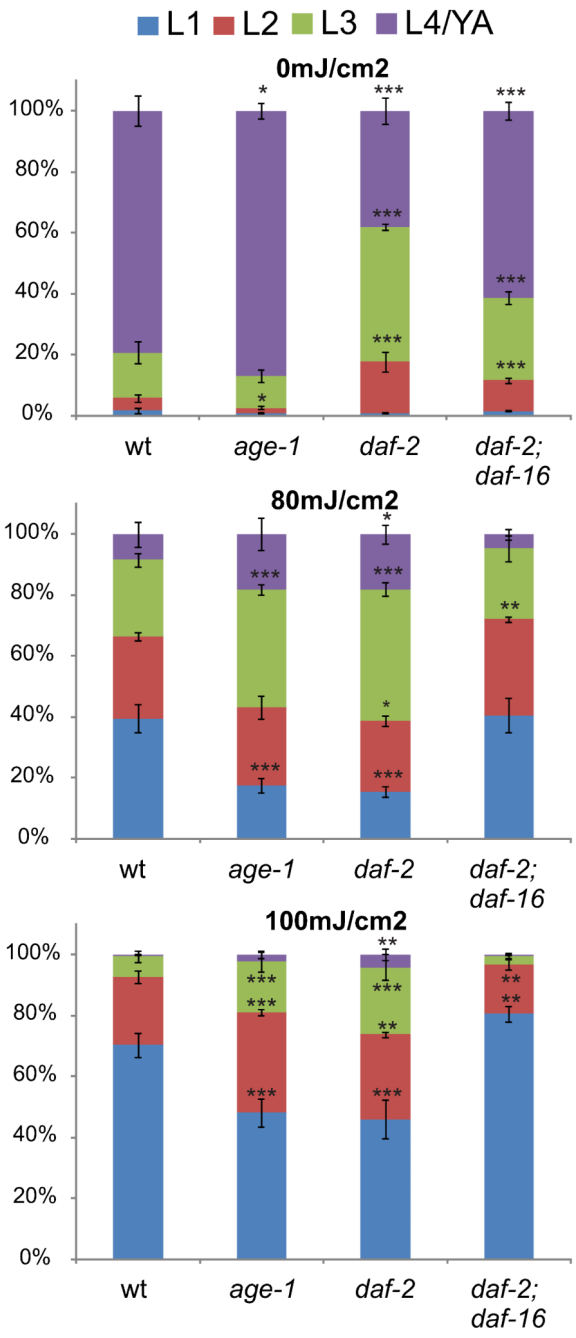

Figure 2. Activation of DAF-16 promotes developmental growth upon UV-induced damage

daf-2 and *age-1* mutants show reduced developmental arrest in a *daf-16* dependent manner. L1 larvae were treated with UV and larval stages determined 48h post treatment. Animals that proceeded to L4 and young adulthood (YA) are scored together. Note that *daf-16* single mutant alleles are analysed in suppl. Figure 2E. (Average of n=4 independent experiments per strain and dose is shown, >1450 individuals analysed per experiment; error bars=SD, *=p<0.05, **=p<0.01, ***=p<0.001, two-tailed T-Test, compared to wt).

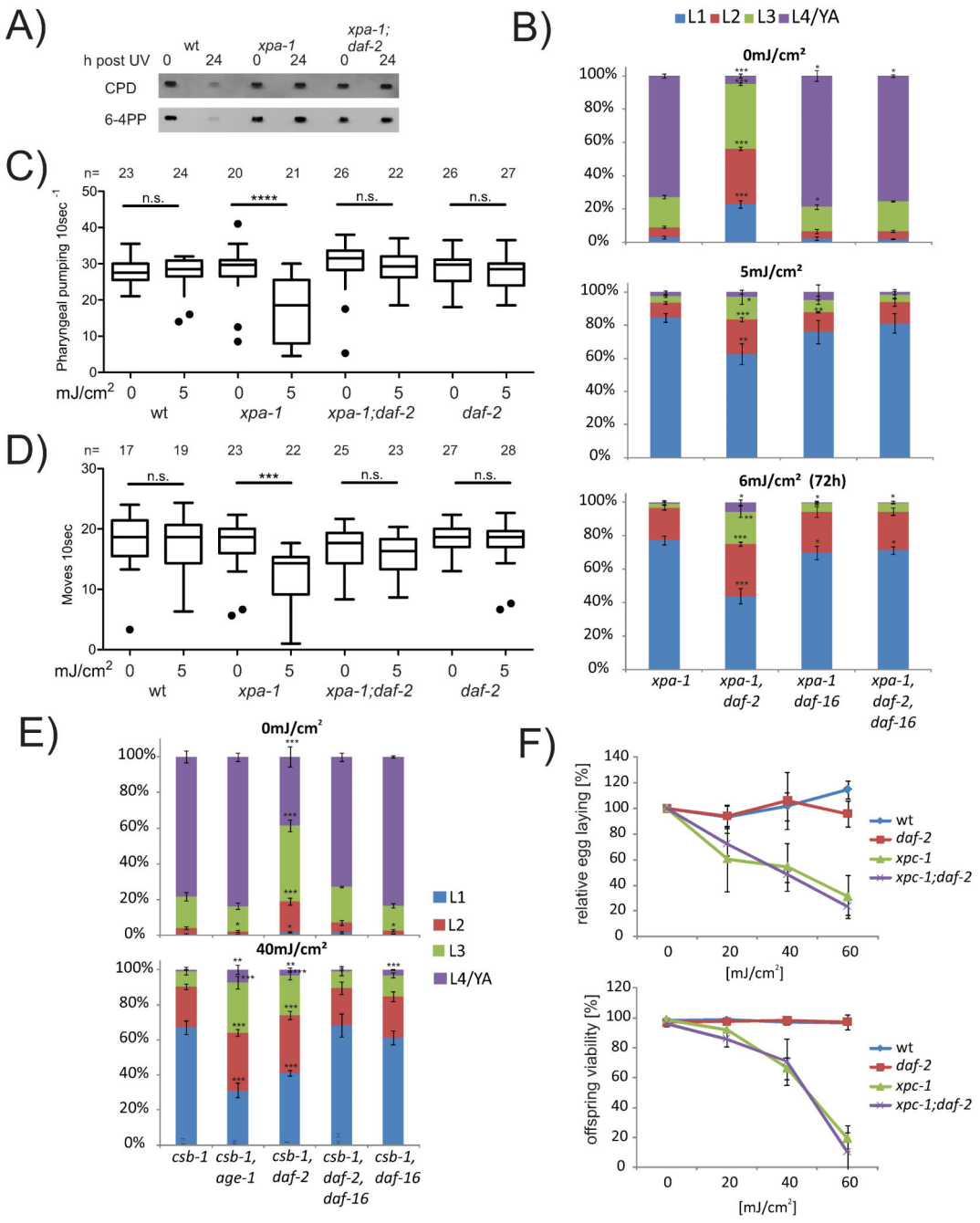

Figure 3. IIS mutants enhance somatic resistance to persistent DNA damage

(A) UV-induced DNA lesions remain unrepaired in *xpa-1* and in *xpa-1;daf-2* mutants. wt, *xpa-1*, and *xpa-1;daf-2* were treated at L1 stage and CPD and 6-4PP lesions were measured by antibody staining in slot blots of worm extracts directly upon treatment with 40mJ/cm^2 UV and 24h later (representative result is shown and the experiment was repeated 3 times) (B) L1 larvae were irradiated or mock treated and developmental stages evaluated 48h or 72h (lower panel) later (average of n=3 independent experiments per strain and dose is shown, >829 individuals analysed per experiment; error bars=SD; *=p<0.05, **=p<0.01,

***=p<0.001, two-tailed T-Test compared to wt) (C) Worms were isolated as L4s and irradiated 24hs later or mock treated and pharyngeal pumping rate per 10 seconds was determined on day 7 after the irradiation (representation in box-and-whisker graph with whiskers 1.5x IQR, ****=p<0.0001, two-tailed T-Test). (D) For body bends measurements, worms were isolated as L4s and irradiated 24hs later or mock treated and body bend rate per 10 seconds was determined on day 8 after the irradiation (representation in box-and-whisker graph with whiskers 1.5x IQR, ***=p<0.001, two-tailed T-Test). (E) L1 larvae were treated and developmental stages assessed 48h post treatment (average of n=3 independent experiments per strain and dose is shown, >3400 individuals analysed per experiment; error bars=SD, *=p<0.05, **=p<0.01, ***=p<0.001, two-tailed T-Test, compared to *csb-1*). (F) L4 larvae were irradiated and were allowed to lay eggs for 5 hours starting at 24h after treatment (F; upper panel; average of n=3 independent experiments per strain and dose, 3 individuals analysed per experiment, error bars=SD). Viable offspring was counted (F; lower panel) 48h post egg-laying (average of n=3 independent experiments per strain and dose shown, offspring of 3 parental individuals analysed per experiment; error bars=SD).

Europe PMC Funders Author Manuscripts

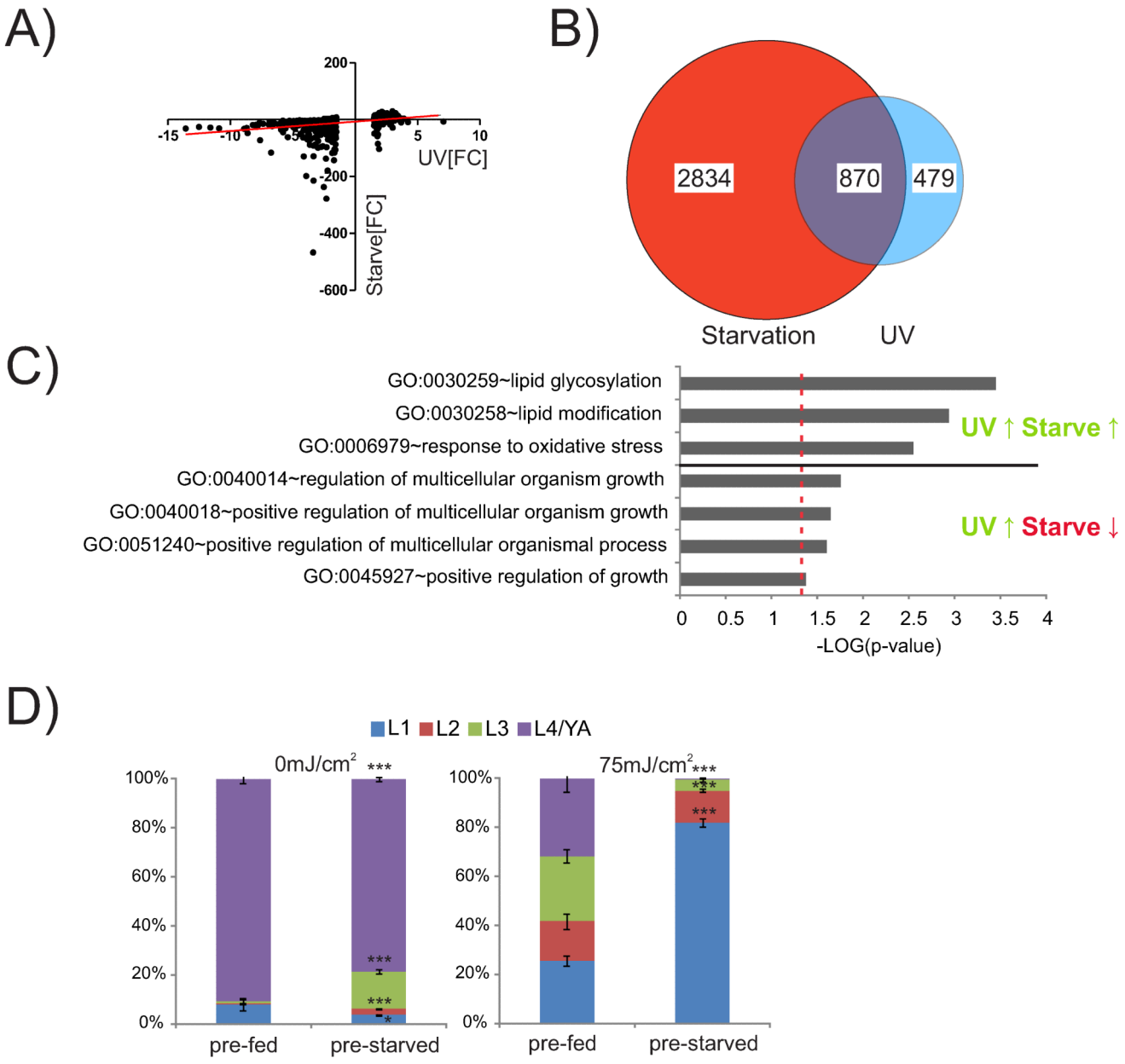

Figure 4. Distinct and similar responses to persistent DNA damage and starvation

Synchronized L1 worms were fed for 4 hours or left under starvation. Starvation responses were previously shown to be quickly reverted upon feeding[24]. Fed wild type worms were treated with 60 mJ/cm^2 UV and compared to non-UV treated controls. (A) xy blot of fold changes of significantly differentially expressed genes in UV treated and starved wt worms; linear regression is depicted in red. (B) Venn diagram showing overlap between significantly differentially expressed genes in response to starvation and UV treatment. (C) Functional clustering of genes that were up- or downregulated upon UV treatment ($p<0.01$, $FC>\pm1.5$) or starvation ($p<0.01$, $FC>\pm2$) reveals significantly overrepresented biological processes. (D) Synchronized L1 larvae were either fed for four hours or left under starvation

and exposed to UV treatment. Upon UV treatment larvae were provided with food and developmental stages were assessed 48h post UV irradiation (average of n=3 independent experiments is shown, >796 individuals analysed per experiment; error bars=SD, ***=p<0.001, two-tailed T-Test).

Europe PMC Funders Author Manuscripts

Europe PMC Funders Author Manuscripts

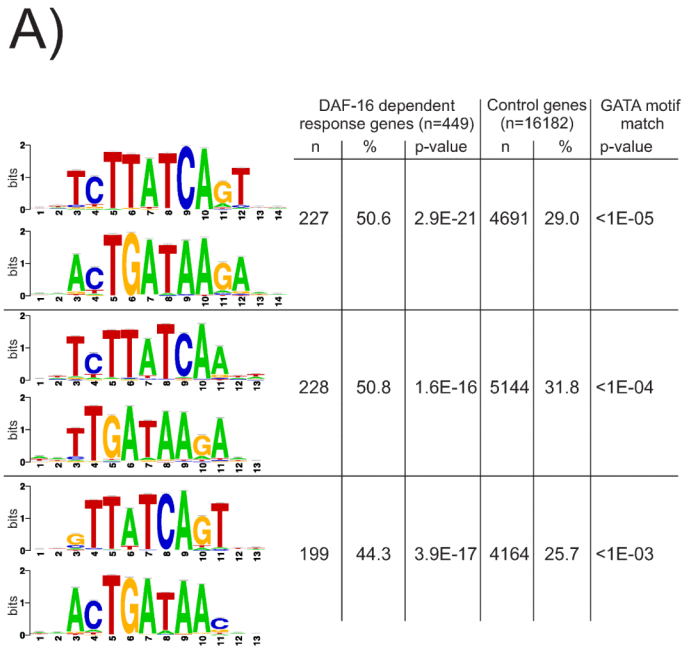

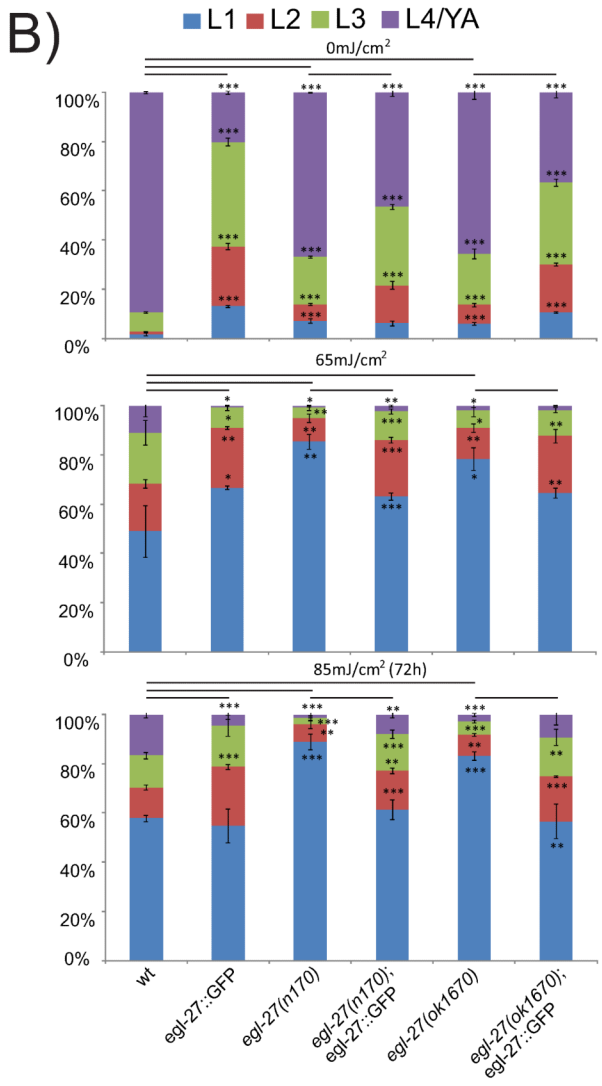

Figure 5. The GATA transcription factor EGL-27 promotes developmental growth upon DNA damage

(A) Specifically 3 GATA motifs are significantly enriched in promoters of DAF-16 dependently induced genes in response to DNA damage. RSAT analysis identified three motifs that were significantly enriched in 1000 bp upstream sequences of 449 (RSAT eligible out of 514 total; see methods) genes that were significantly induced in *daf-2* mutants (FC>1.5; p<0.01) upon UV and more strongly induced upon DNA damage in *daf-2 vs. daf-2;daf-16*, *daf-2 vs. wt*, and *wt vs. daf-16*. Motif comparisons with transcription factors databases identified significant match to GATA motifs. (B) *egl-27(n170)* and *egl-27(ok1670)* mutants are hypersensitive to larval arrest following DNA damage and rescued by transgenic *egl-27::GFP* expression. Synchronized L1 larvae were exposed to UV and larval stages assessed 48h post treatment (average of n=3 independent experiments per strain and dose is shown, >900 individuals analysed per experiment; error bars=SD *=p<0.05, **=p<0.01, ***=p<0.001, two-tailed T-Test).

Europe PMC Funders Author Manuscripts

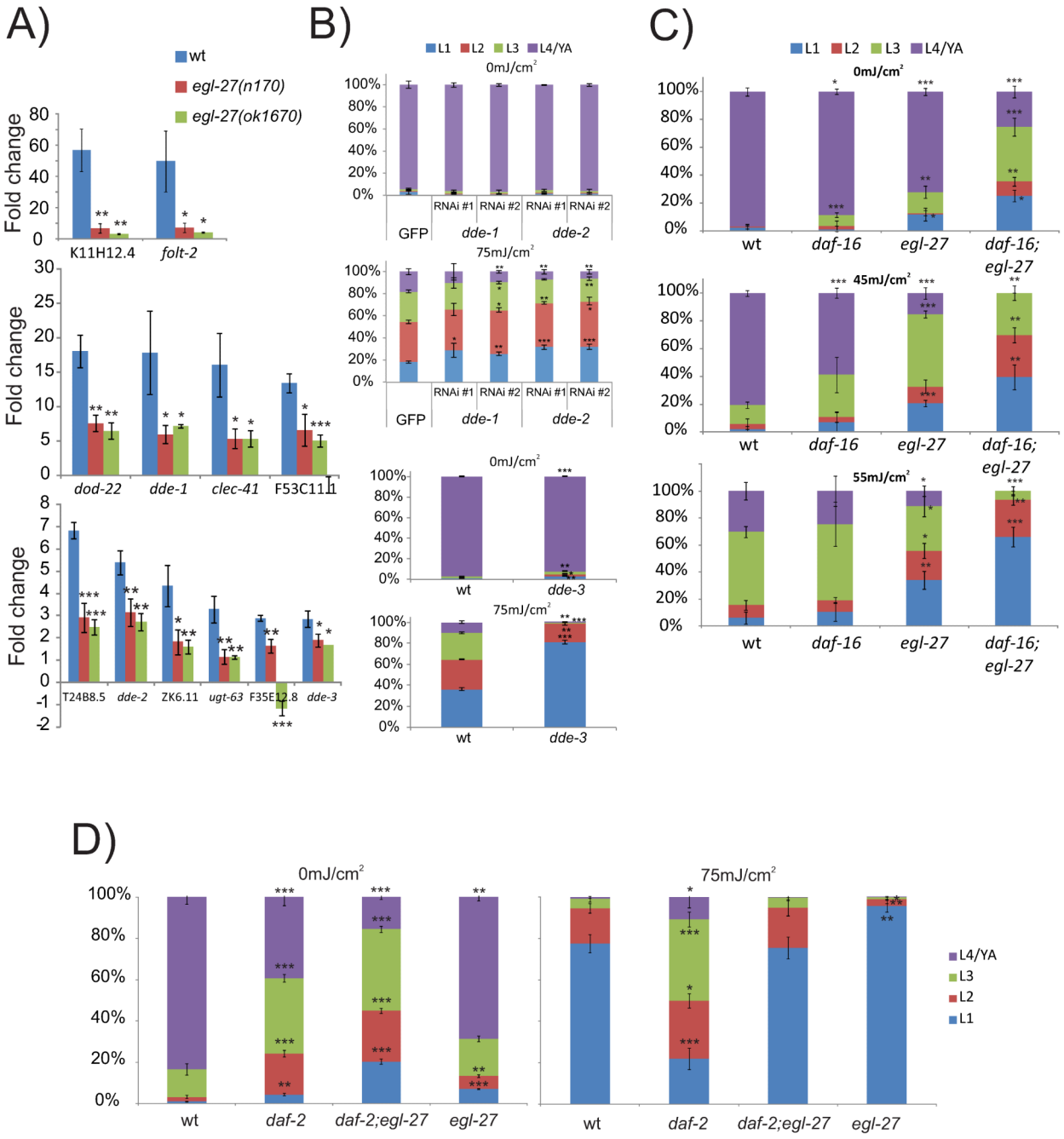

Figure 6. The GATA transcription factor EGL-27 co-regulates DAF-16 target genes and acts downstream of DAF-2 to promote developmental growth in response to DNA damage

(A) *egl-27* is required for DAF-16 target gene induction. Genes that were defined as DAF-16 dependently induced (see Figure legend 5A) were analysed by qPCR 6h post UV in wt, *egl-27(n170)*, and *egl-27(ok1670)* mutants (average of n=3 independent experiments). (B) RNAi knockdown of "DNA damage effector downstream of DAF-16 and EGL-27" dde-1 and *dde-2* by two independent RNAi constructs (RNAi #1[52], RNAi #2[53]) and a genetic mutation in *dde-3(gk696370)* lead to enhanced UV sensitivity (*dde-3* mutant was

outcrossed prior to analysis; average of n=3 independent experiments per strain and dose is shown, >211 individuals analysed per experiment; error bars=SD; *=p<0.05, **=p<0.01, ***=p<0.001, two-tailed T-Test, compared to GFP RNAi or wt, respectively). (C) wt, *daf-16*, *egl-27* and *daf-16;egl-27* upon UV treatment were analysed 48h post UV (average of n=3 independent experiments per strain and dose is shown, >25 individuals analysed per experiment analysed; error bars=SD; *=p<0.05, **=p<0.01, ***=p<0.001, two-tailed T-Test compared to wt). (D) *egl-27* suppresses UV tolerance of *daf-2*. Synchronized L1 larvae were UV treated and developmental stages assessed 48h post treatment (average of n=3 independent experiments per strain and dose is shown, >1738 individuals analysed per experiment; error bars=SD, *=p<0.05, **=p<0.01, ***=p<0.001, two-tailed T-Test compared to wt).

Europe PMC Funders Author Manuscripts

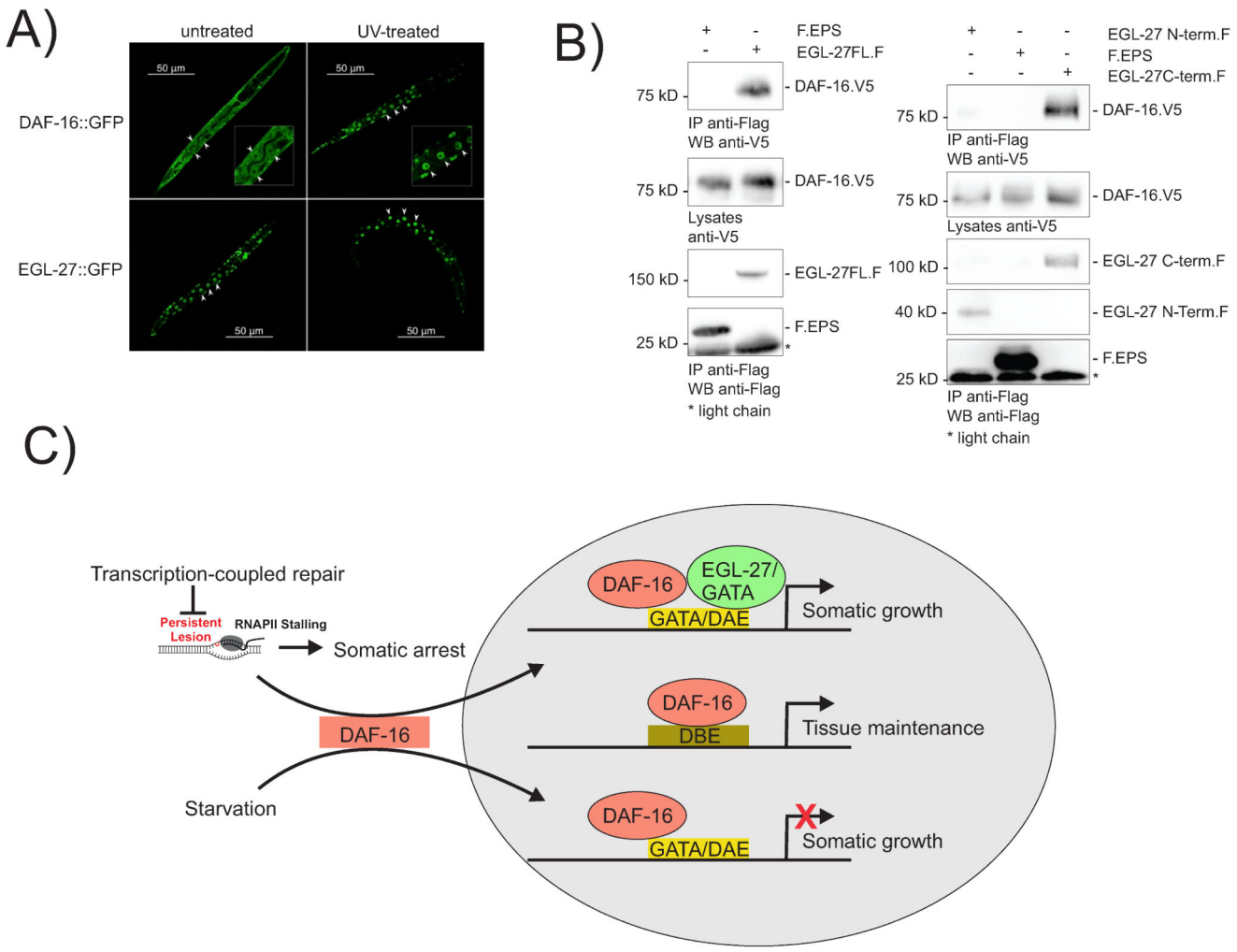

Figure 7. EGL-27 interacts with DAF-16 upon DNA damage

(A) DAF-16::GFP upon UV treatment co-localizes with EGL-27::GFP in the nucleus of intestinal cells. L1 synchronized larvae were fed and UV-treated with 150 mJ/cm^2 and kept at 20°C, images were taken 6hs after. Upper panels show DAF-16::GFP worms, left panel non-UV treated and right panel a completely nuclear DAF-16::GFP UV-irradiated worm. Lower panels show EGL-27::GFP worms, left panel non-UV treated and right panel UV-irradiated (representative images shown; experiment repeated at least 3 times). (B) EGL-27 interacts with DAF-16 (left panel). HEK293T cells were transiently transfected and after immunoprecipitation (IP) with FLAG (M2) beads, Western blot analysis revealed that DAF-16.V5 coprecipitated with EGL-27.FLAG but not with a control protein (EPS) (representative result of 4 independent experiments). Interaction with DAF-16 is mediated by the C-terminal part of EGL-27 (right panel). HEK293T cells were transiently transfected and after IP with FLAG (M2) beads, Western blot analysis revealed that DAF-16.V5 co-precipitated with the EGL-27 C-terminus but not with an N-terminal truncation or a control protein (EPS) (representative result of 4 independent experiments). (C) Model for the differential consequences of DAF-16 activation upon persistent DNA damage and upon starvation. In response to persistent DNA lesions in somatic tissues DAF-16 activation

Europe PMC Funders Author Manuscripts

results in induction of somatic growth genes, which are repressed by DAF-16 upon starvation, through recognition of DAE promoter elements through the GATA transcription factor EGL-27. In both cases stress response genes are induced through recognition of DBE motifs leading to enhanced tissue maintenance.

Europe PMC Funders Author Manuscripts

Table 1

Promoter analysis reveals overrepresentation of distinct DAF-16 response elements among UV and starvation response genes

All genes that neither responded to UV nor starvation were used as controls. Analysis was restricted to annotated non-redundant genes (Suppl. Table 8). To validate the approach we used a published dataset of DAF-16 regulated genes in adult worms[26] (bottom two rows).

GENE RESPONSE GROUP			DBE DAF-16 Binding Element		DAE DAF-16 Associated Element	
			TGTTTAC	p-value	CTTATCA	p-value
↑ UV (n=497)			17.3	2.4E-03	36.6	1.6E-18
↓ UV (n=595)			14.0	2.8E-01	22.6	3.6E-02
↑ UV (non-overlapped) (n=156)			16.0	1.8E-01	42.9	3.4E-11
↓ UV (non-overlapped) (n=270)			15.2	1.9E-01	24.4	2.5E-02
↑ STARVATION (n=1531)			18.6	1.3E-10	22.8	1.0E-03
↓ STARVATION (n=1385)			12.4	1.0E+00	23.0	8.3E-04
↑ STARVATION (non-overlapped) (n=1338)			18.0	3.4E-08	22.4	4.9E-03
↓ STARVATION (non-overlapped) (n=881)			12.5	1.0E+00	22.2	2.3E-02
Overlapped (n=697)			15.2	4.0E-02	24.7	8.7E-04
UV↑	ST↑	(n=163)	25.8	4.3E-06	25.8	4.6E-02
UV↑	ST↓	(n=98)	10.2	6.4E-01	43.9	3.4E-08
UV↓	ST↑	(n=30)	6.7	5.8E-01	23.3	3.6E-01
UV↓	ST↓	(n=406)	12.8	8.2E-01	19.7	4.6E-01
Control (n=13298)			12.5		19.4	
daf-2(−) induced	(n=231)		24.2	1.15E-06	38.5	2.1E-11
daf-2(−) repressed	(n=220)		15.5	6.25E-02	38.6	4.9E-11